APPENDIX I. MAGNETIC AND GRAVITY DATA BETWEEN JAPAN AND SURVEY AREA, AND BETWEEN SURVEY AREA AND HAWAIIAN ISLANDS

Takemi Ishihara and Kensaku Tamaki

Magnetic and gravity measurements were continuously carried out between Japan and the survey area, and between the survey area and the Hawaiian Islands. Tracks are shown in Fig. AI-1, and some positions along the tracks which are cited in the later figures are plotted in that figure and also are listed in Table AI-1. Data processing of magnetic and gravity anomalies was done in the same way as described in Chapter VI and V respectively.

Results

Magnetic and gravity anomaly profiles obtained are shown together with bathymetric data in Figs. AI-2—18.

North of the Izu-Ogasawara area, magnetic anomalies with a peak to peak amplitude of about 1000 γ and with an apparent wavelength of about 100 km were observed (Fig. AI-2). Free air anomalies over the Ogasawara Ridge have a maximum of nearly 300 mgal. However, from the Shichito-Iojima Ridge to the Nishi-Shichito Ridge, no anomalies greater than 100 mgal are found, inspite of the fact that they exist beneath approximately the same water depth (Fig. AI-3). On the other hand, magnetic anomalies from the Shichito-Iojima Ridge to the Nishi-Shichito Ridge including the trough between them have about the same order of peak to peak amplitude (150–200 γ)

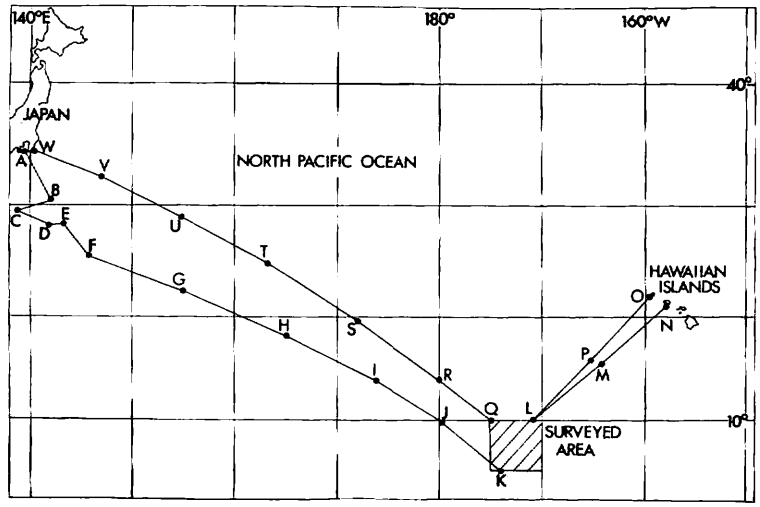

Fig. AI-1 Track of magnetic and gravity survey between Japan and the survey area and between the survey area and the Hawaiian Islands. Positions A to W in Figs. AI-2—18 are also plotted.

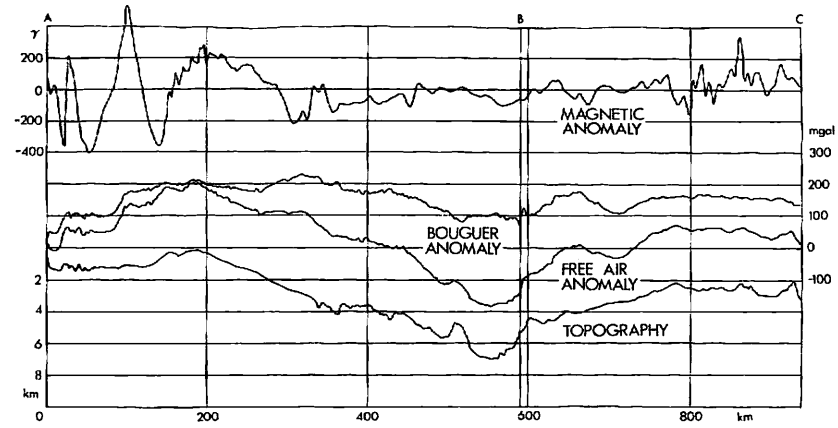

Fig. A1-2 Magnetic and gravity anomaly profile from A to C.

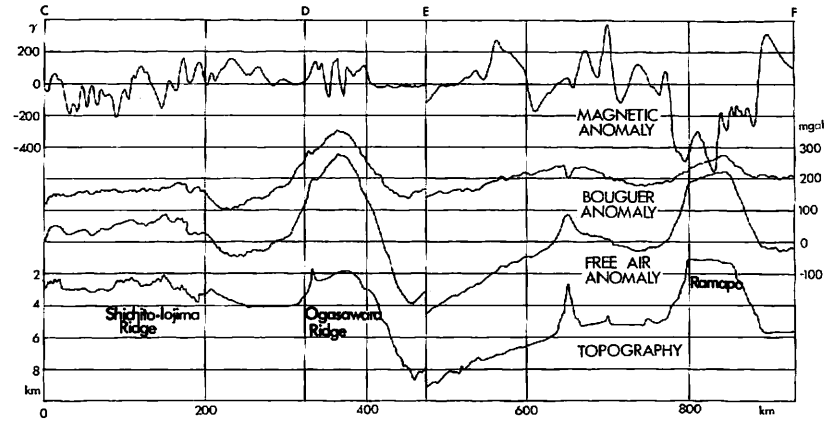

Fig. A1-3 Magnetic and gravity anomaly profile from C to F.

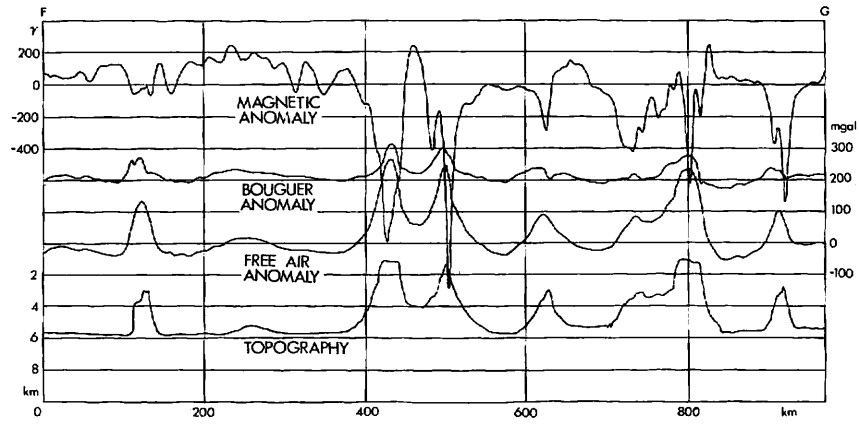

Fig. A1-4 Magnetic and gravity anomaly profile from F to G.

Fig. AI-5 Magnetic and gravity anomaly profile from G to H.

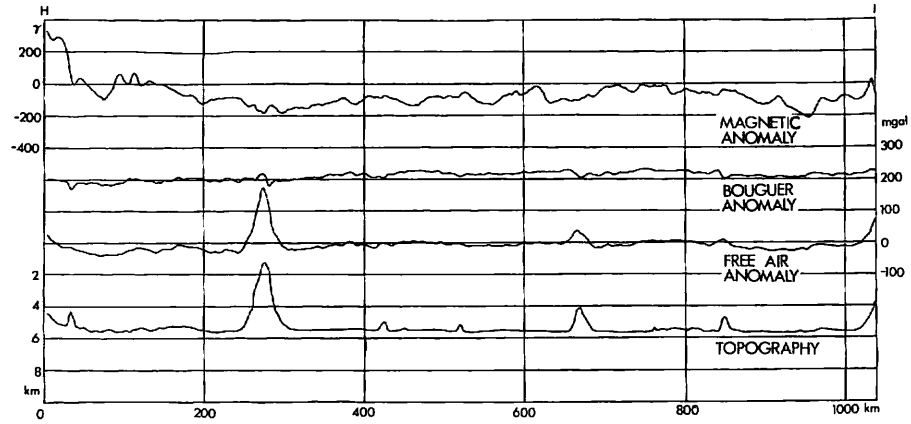

Fig. AI-6 Magnetic and gravity anomaly profile from H to I.

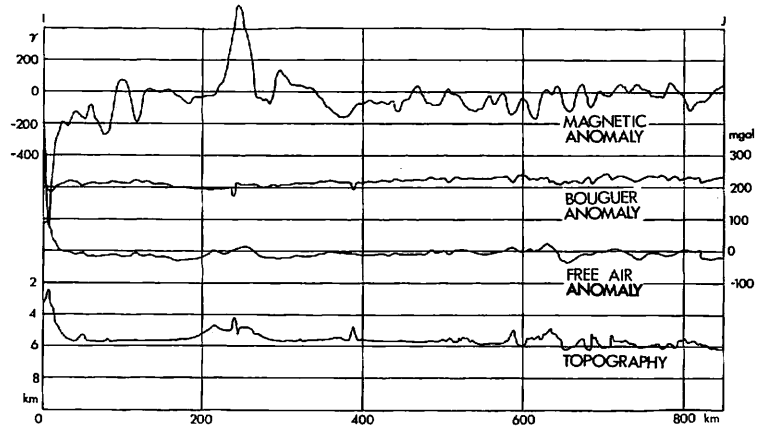

Fig. AI-7 Magnetic and gravity anomaly profile from I to J.

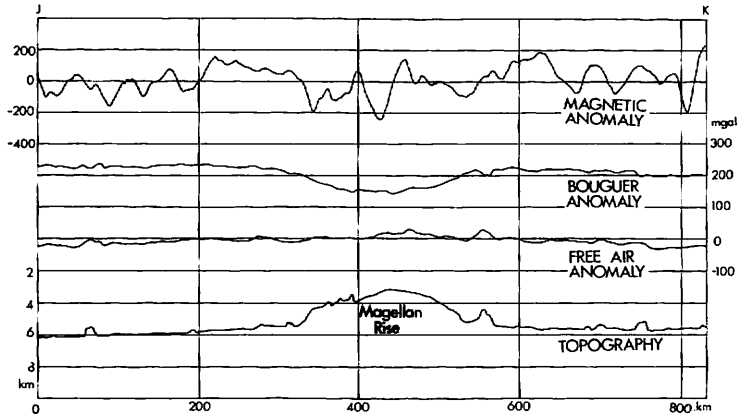

Fig. AI-8 Magnetic and gravity anomaly profile from J to K.

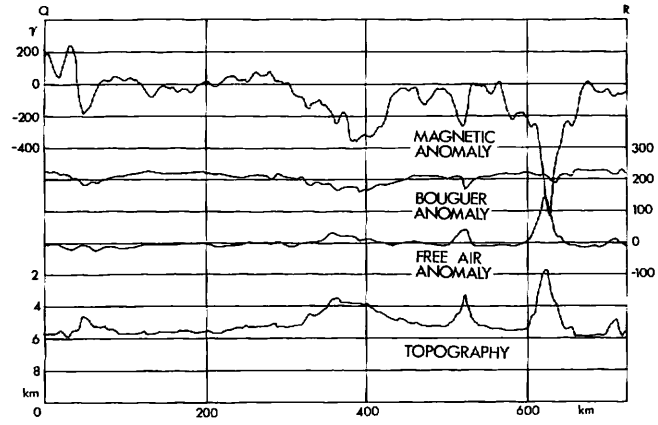

Fig. AI-9 Magnetic and gravity anomaly profile from Q to R.

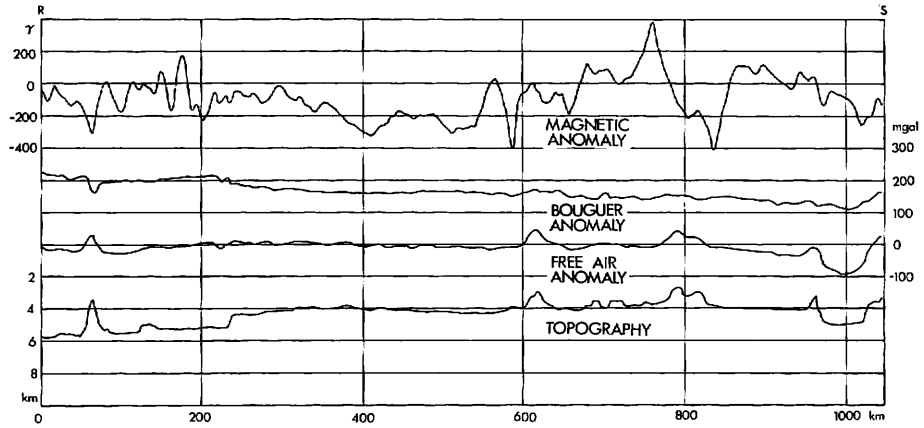

Fig. AI-10 Magnetic and gravity anomaly profile from R to S.

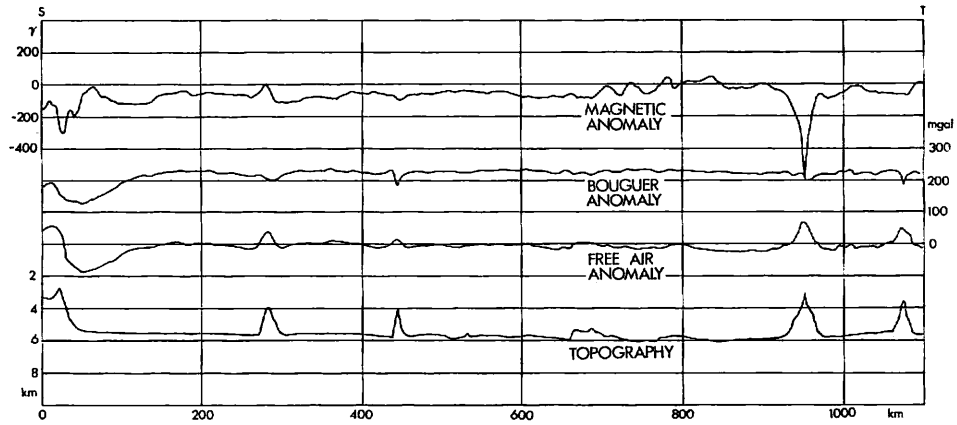

Fig. AI-11 Magnetic and gravity anomaly profile from S to T.

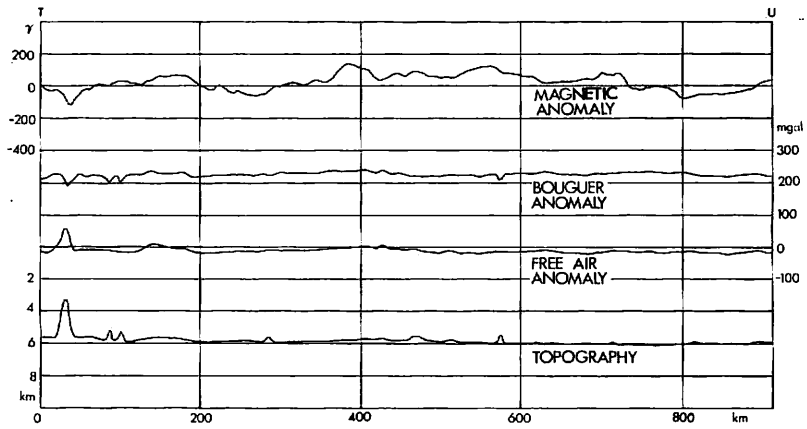

Fig. AI-12 Magnetic and gravity anomaly profile from T to U.

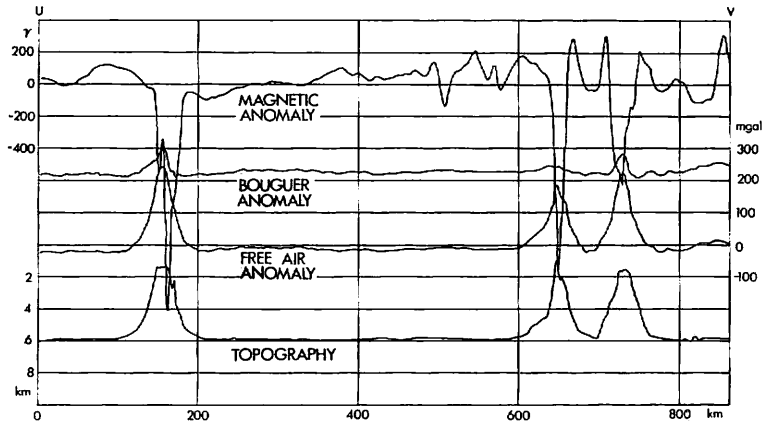

Fig. AI-13 Magnetic and gravity anomaly profile from U to V.

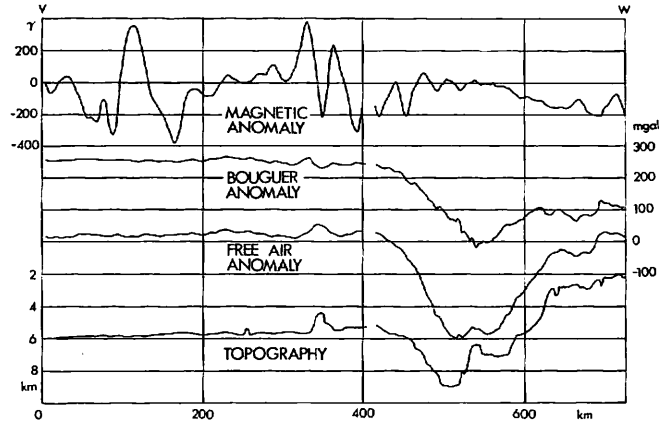

Fig. AI-14 Magnetic and gravity anomaly profile from V to W.

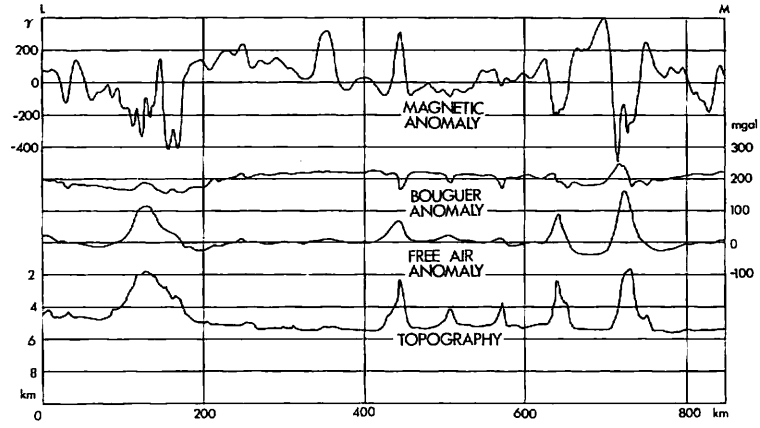

Fig. AI-15 Magnetic and gravity anomaly profile from L to M.

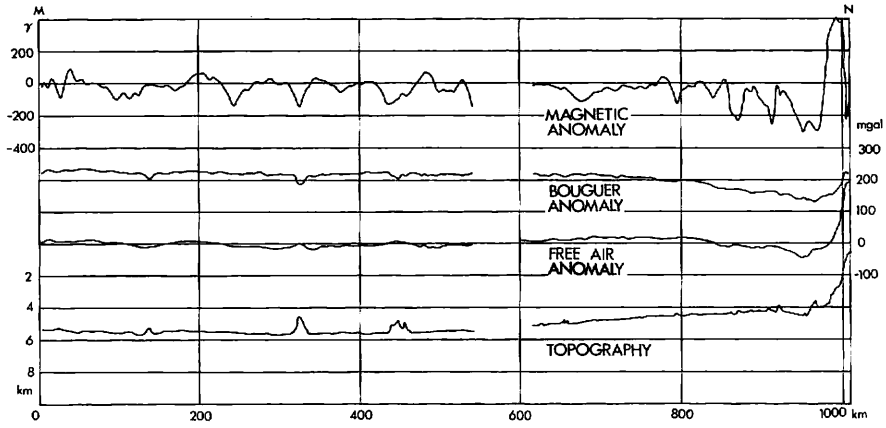

Fig. AI-16 Magnetic and gravity anomaly profile from M to N.

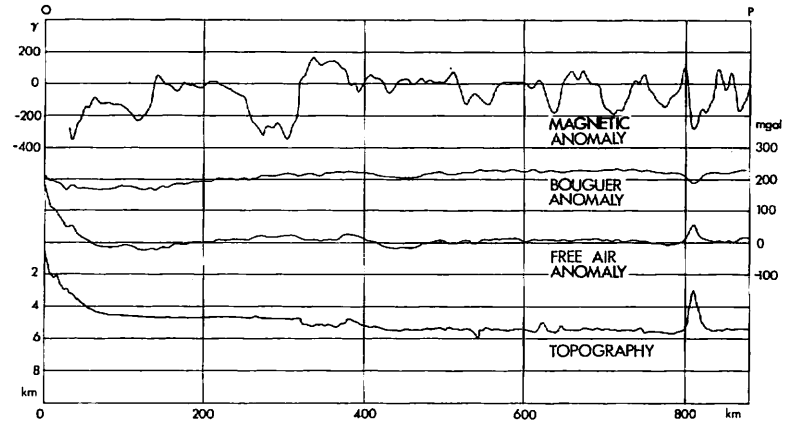

Fig. AI-17 Magnetic and gravity anomaly profile from O to P.

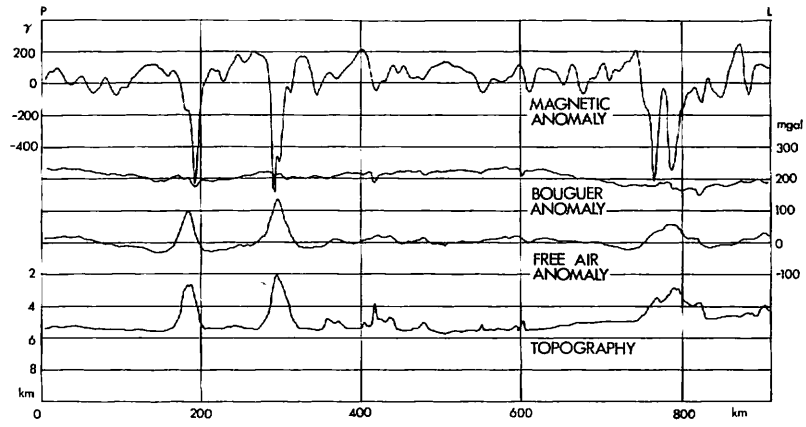

fig. AI-18 Magnetic and gravity anomaly profile from P to L.

and about the same order of apparent wavelength ($\sim$10 km) as those over the Ogasawara Ridge. The Ogasawara Trough is relatively quiet, suggesting thickening of sediment layers.

There are many seamounts beyond the Izu-Ogasawara Trench. Almost all of them are characterized by sharp negative anomalies. Taking into account that normally magnetized seamounts at low latitudes have negative peaks over them, the number of normally magnetized seamounts should be much greater than that of reversally magnetized seamounts. All free air anomaly highs corresponds to seamounts, and some of the seamounts are accompanied with marked negative zones around them, such as observed along the Hawaiian-Emperor Seamount Chain, suggesting deformation of the lithosphere after the birth of the seamounts (WATTS and COCHRAN, 1974).

Magnetic anomalies, which are not correlated with the topography, occur to the east of about 175°E (Fig. AI-7, 8), between the survey area and the Hawaiian Islands (Figs. AI-15 – 18) and just to the east of the Izu-Ogasawara Trench (Figs. AI-13, 14).

Table AI-1 Positions along tracks Japan-survey area and survey area-Hawaii.

	Latitude	Longitude
A	34°58′N	139°12′E
B	30°18′N	142°15′E
C	29°32′N	138°45′E
D	28°19′N	141°47′E
E	28°20′N	143°20′E
E′	28°32′N	143°04′E
F	25°20′N	146°00′E
G	22°26′N	155°00′E
H	18°15′N	165°00′E
I	14°00′N	173°40′E
J	09°48′N	179°48′W
K	05°00′N	174°00′W
L	10°00′N	171°00′W
M	15°00′N	165°05′W
N	21°04′N	157°58′W
O	21°52′N	159°37′W
P	16°00′N	165°15′W
Q	09°59′N	174°45′W
R	14°00′N	180°00′
S	19°30′N	172°00′E
T	24°51′N	163°00′E
U	28°54′N	155°00′E
V	32°29′N	147°00′E
W	34°42′N	139°40′E

Generally speaking, they have small amplitudes (about 200γ peak to peak) and are disturbed by seamounts. They are presumably Mesozoic lineations (LARSON and PITMAN, 1972).

Over the Magellan Rise, which exists just to the west of the survey area, free air anomalies are almost 0 mgal, and magnetic anomalies do not have sharp peaks (Fig. AI-8). From this it is concluded that the Magellan Rise is mainly formed of low density, non-magnetic sediment layers.

References

LARSON, R.L. and CHASE, C. G. (1972) Late Mesozoic evolution of the western Pacific Ocean. *Geol. Soc. Amer. Bull.*, vol. 83, p. 3627–3644.

————and PITMAN III, W. C. (1972) World-wide correlation of Mesozoic magnetic anomalies, and its implications. *Geol. Soc. Amer. Bull.*, vol. 83, p. 3645–3662.

WATTS, A. B. and COCHRAN, J. R. (1974) Gravity anomalies and flexure of the lithosphere along the Hawaiian-Emperor Seamount Chain. *Geophys. J. R. astr. Soc.*, vol. 38, p. 119–141.